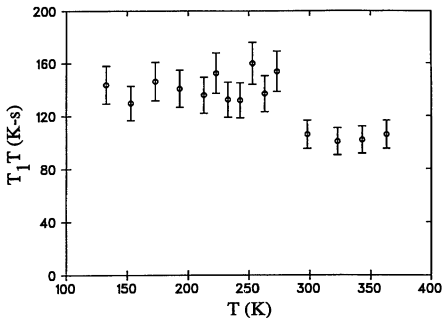

Fig. 4. Temperature dependence of the ^{13}C spin-lattice relaxation time T_1 in K_3C_{60}, plotted as T_1T versus T. Error bars are standard deviations estimated from five T_2 measurements at 298 K.

expression for spin-lattice relaxation by a contact hyperfine interaction (*16*),

$$\frac{1}{\kappa} = \frac{64}{9}\pi^3 k\hbar^3\gamma_e^2\gamma_n^2|\Psi(0)|^4\rho^2(E_f) \quad (1)$$

where γ_e and γ_n are the gyromagnetic ratios of the electron and the ^{13}C nucleus, we calculate the local electron density of states at the Fermi level and at a carbon nucleus in the normal state of K_3C_{60} to be $|\Psi(0)|^2\rho(E_f) = 7.6 \times 10^{24}$ eV^{-1} cm^{-3} per C_{60}^{3-} ion. We estimate $|\Psi(0)|^2$, the average electron density at a carbon nucleus for an orbital at the Fermi level (normalized to 1 for each C_{60} molecule), to be of order 4×10^{23} cm^{-3}. This value is determined from unrestricted Hartree-Fock calculations of the ratio of the unpaired spin density in carbon 2*s* orbitals in C_{60}^{3-} to that in planar methyl radical (*17*) and from the measured isotropic ^{13}C hyperfine coupling in methyl radical (*18*). 2*s*-2*p* hybridization (*19*) associated with the nonplanarity of C_{60} and core polarization make comparable contributions to $|\Psi(0)|^2$. We then derive a density of states at the Fermi level $\rho(E_f) = 20$ eV^{-1} per C_{60}^{3-} ion.

We interpret the 43 ppm downfield shift of the K_3C_{60} ^{13}C NMR resonance relative to the C_{60} resonance to be primarily a Knight shift attributable to hyperfine coupling between ^{13}C nuclei and conduction electron spins. A downfield shift of only 14 ppm relative to neutral C_{60} has been observed for a diamagnetic C_{60} anion of unknown charge in solution (*20*), suggesting a small orbital contribution to the shift in K_3C_{60}. With $\kappa = 140$ K-s, the Korringa relation for a Fermi gas of noninteracting electrons predicts a ^{13}C Knight shift of 170 ppm. The discrepancy between the observed and predicted shifts raises the possibility that orbital couplings (*21*) make a substantial contribution to the relaxation rate.

In conclusion, our ^{13}C NMR spectra of K_xC_{60} provide strong evidence for phase separation in material with $0 < x < 3$. The NMR lineshapes demonstrate the presence of rapid, large amplitude molecular reorientations at room temperature in K_3C_{60} and the absence of such reorientations in K_6C_{60}. NMR relaxation measurements indicate the central role played by C_{60}^{3-} ions in the conductivity of K_3C_{60} and suggest that ^{13}C NMR will be an important probe of the superconducting state of K_3C_{60} and other alkali fullerides. Further low temperature measurements are in progress.

Note added in proof: We find the ^{13}C NMR T_1T to be 69 ± 8 K-s in Rb_3C_{60} between 213 K and 344 K, indicating that $\rho(E_f)$ is 40% larger than K_3C_{60}.

REFERENCES AND NOTES

1. R. C. Haddon *et al.*, *Nature* **350**, 320 (1991).
2. A. F. Hebard *et al.*, *ibid.*, p. 600.
3. M. J. Rosseinsky *et al.*, *Phys. Rev. Lett.* **66**, 2830 (1991).
4. H. W. Kroto, J. R. Heath, S. C. O'Brien, R. F. Curl, R. E. Smalley, *Nature* **318**, 162 (1985).
5. W. Krätschmer, L. D. Lamb, K. Fostiropoulos, D. R. Huffman, *ibid.* **347**, 354 (1990).
6. P. W. Stephens, *et al.*, *ibid.* **351**, 632 (1991).
7. O. Zhou *et al.*, *ibid.*, p. 462.
8. K. Holczer, *Science* **252**, 1154 (1991).
9. C. S. Yannoni, R. D. Johnson, G. Meijer, D. S. Bethune, J. R. Salem, *J. Phys. Chem.* **95**, 9 (1991).
10. R. Tycko *et al.*, *ibid.*, p. 95.
11. R. Taylor, J. P. Hare, A. K. Abdul-Sada, H. W. Kroto, *J. Chem. Soc. Chem. Comm.* **1990**, 1423 (1990).
12. R. M. Fleming *et al.*, *Mat. Res. Soc. Proc.*, in press.
13. R. Tycko *et al.*, *Phys. Rev. Lett.*, in press.
14. P. A. Heiney *et al.*, *ibid.* **66**, 2911 (1991).
15. R. E. Haufler *et al.*, *Chem. Phys. Lett.* **179**, 449 (1991).
16. C. P. Slichter, *Principles of Magnetic Resonance* (Springer-Verlag, New York, ed. 3, 1990).
17. K. Raghavachari, unpublished results.
18. R. W. Fessenden, *J. Phys. Chem.* **71**, 74 (1967).
19. R. C. Haddon, *J. Am. Chem. Soc.* **109**, 1676 (1987).
20. J. W. Bausch *et al.*, *ibid.* **113**, 3205 (1991).
21. J. Winter, *Magnetic Resonance in Metals* (Oxford Univ. Press, London, 1971).

22. We thank S. M. Zahurak, A. V. Makhija, and R. C. Haddon for supplying purified C_{60}, M. F. Needels for providing a program for Madelung calculations, and R. C. Haddon, K. Raghavachari, R. E. Walstedt, and M. Schluter for valuable suggestions.

15 July 1991; accepted 26 July 1991

$(Rb_xK_{1-x})_3C_{60}$ Superconductors: Formation of a Continuous Series of Solid Solutions

CHIA-CHUN CHEN, STEPHEN P. KELTY, CHARLES M. LIEBER*

By means of an approach that employs alkali-metal alloys, bulk single-phase $(Rb_xK_{1-x})_3C_{60}$ superconductors have been prepared for all x between 0 and 1. For $x = 1$ it is shown that the maximum superconducting fraction, which approaches 100% in sintered pellets, occurs at a Rb to C_{60} ratio of 3:1. More importantly, single-phase superconductors are formed at all intermediate values of x, and it is shown that the transition temperature (T_c) increases linearly with x in this series of materials. The formation of a continuous range of solid solutions demonstrates that the rubidium- and potassium-doped C_{60} superconducting phases must be isostructural, and furthermore, suggests that the linear increase in T_c with x results from a chemical pressure effect.

THE RECENT FINDING OF SUPERCONductivity in K-doped C_{60} (*1*) has been followed by an intense effort directed toward understanding the chemistry and physics of alkali metal–doped C_{60} solids (*2–12*). In particular, studies of the K-doped superconducting phase, K_3C_{60}, have yielded insight into the structure (*8*), coherence length and penetration depth (*11*), and pressure dependence of T_c (*9, 10*). The success of these physical measurements has in large part been due to the development of a method for preparing K-doped C_{60} samples that contain predominantly the superconducting phase (*4*). In the case of Rb_xC_{60}, which has a significantly higher transition temperature (T_c) than K_3C_{60} (28 versus 18 K), the reported yields of superconducting phase have been much lower, and thus have precluded the clear identification of the composition and key properties of this superconducting phase.

Understanding the origin of superconductivity in doped C_{60} will require, however, experimentalists to characterize the properties of other alkali metal–doped C_{60} superconductors, and importantly to elucidate the relationship between these phases. To this end we have undertaken the study of C_{60} doped simultaneously with Rb and K, and herein report the synthesis and characterization of bulk superconducting $(Rb_xK_{1-x})_3C_{60}$ materials for $x = 0$ to 1. In previous studies of M_xC_{60} materials most researchers have relied upon the direct reaction of alkali-metal vapor with C_{60} (*1–4*). While this approach results in the formation of high yields of K_3C_{60} (*4*), only small fractions of Rb-doped and no Cs-doped C_{60} superconducting phase fabricated with this method have been reported (*3, 4*). To enable greater control

Department of Chemistry and Division of Applied Sciences, Harvard University, Cambridge, MA 02138.

*To whom correspondence should be addressed.

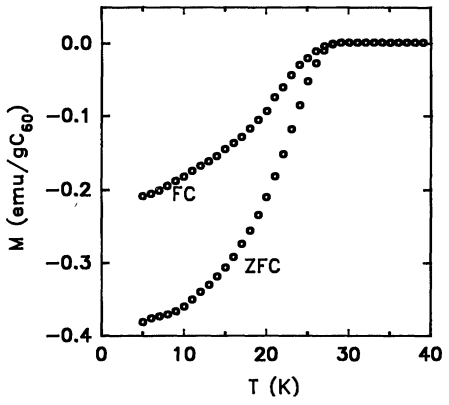

Fig. 1. Temperature dependence of the magnetization obtained for a Rb_3C_{60} powder sample. The curves were recorded by cooling in a zero field to 5 K and subsequent warming in a 50-Oe field (ZFC) and by cooling in a 50-Oe field from above T_c (FC). The large value of flux expulsion (Meissner effect), which exceeds 50% of the ZFC value, indicates that the sample is a homogeneous bulk superconductor.

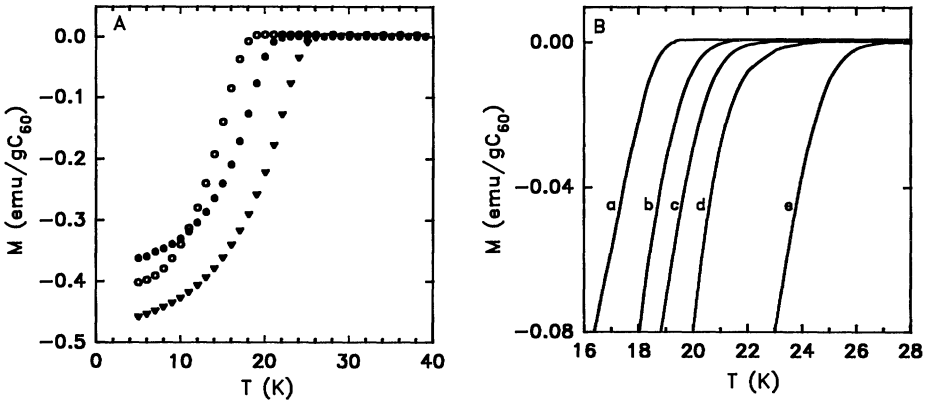

Fig. 3. (**A**) Temperature dependence of the magnetization recorded on $x = 0$ (○), $x = 0.5$ (●), and $x = 0.9$ (▲) powder samples of $(Rb_xK_{1-x})_3C_{60}$. The low-temperature shielding values for these ZFC curves show that the superconducting fraction is > 35%. (**B**) ZFC curves recorded over a limited temperature range to highlight the systematic variation of T_c with x; curves a, b, c, d, and e correspond to $x = 0.1$, 0.25, 0.5, 0.75, and 0.9, respectively. At least 7 mg of C_{60} was used to prepare each of these samples.

of the doping process we have developed an approach that utilizes alloys of the alkali metals, and have recently demonstrated the effectiveness of this method by preparing the previously unknown Cs_xC_{60} superconducting phase (*12*). In this report we have used alloys of the type $Rb_xK_{1-x}M$ (M = Hg, Tl) to dope C_{60}. For $x = 1$ we show that the maximum diamagnetic shielding signal, which approaches 100% in sintered pellets, occurs at a Rb to C_{60} ratio of 3:1. More importantly, we demonstrate for all intermediate values of x that single phase $(Rb_xK_{1-x})_3C_{60}$ superconductors are formed and that T_c increases linearly with x in these materials. The formation of a continuous range of solid solutions demonstrates chemically that the Rb- and K-doped C_{60} superconducting phases must be isostructural.

C_{60} was synthesized in a stainless steel chamber with high-purity graphite electrodes (99.9995%) (*13, 14*). The carbon soot was extracted with benzene, and pure C_{60} was obtained from this solution by chromatography on neutral alumina (*15*). The purification and isolation were carried out in the dark to minimize impurities from the photodegradation of C_{60}. The C_{60} was then dried under vacuum at 250°C for several hours to remove solvent. $Rb_xK_{1-x}Hg$ alloys were made by melting the desired ratio of high purity metals in an inert atmosphere glove box equipped with an O_2/H_2O removal system. In general, samples were prepared by grinding the desired ratio of C_{60} and $Rb_xK_{1-x}Hg$ in the glove box, and then sealing the resulting powder in a quartz tube on a vacuum-line without exposure to air; 8 to 10 mg of C_{60} was typically used for each reaction. Samples were heated isothermally (200° to 250°C) and the magnetization was determined as a function of reaction time with the use of superconducting quantum interference device (SQUID) magnetometer (MPMS2, Quantum Design, San Diego, California). Samples typically exhibit significant diamagnetic shielding (that is, superconducting phase) after 1 hour of reaction. The superconducting fraction continues to increase with reaction time and reaches a maximum after 48 to 72 hours.

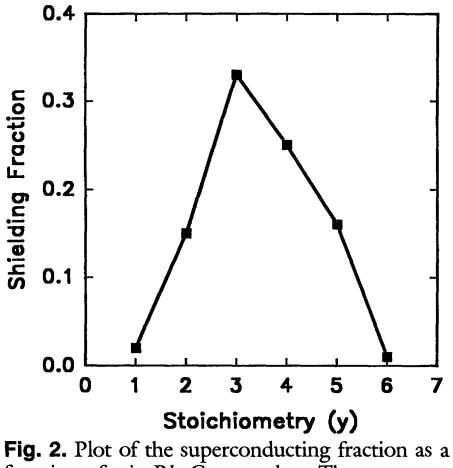

Fig. 2. Plot of the superconducting fraction as a function of y in Rb_yC_{60} powders. The superconducting fraction was determined from the diamagnetic shielding value at 5 K. The data points correspond to maximum yield at each composition.

Temperature-dependent magnetic susceptibility measurements were obtained from a (Rb-Hg):C_{60} 3:1 sample (Fig. 1). The sample was made up from 11.8 mg of RbHg and 10.1 mg of C_{60}, and was reacted at 200°C for 96 hours; following this reaction Hg metal was observed in the sample tube. The shielding (flux exclusion) curve obtained by cooling the sample in zero field to 5 K and then warming in a field of 50 Oe shows a clear transition at 28 K. The corresponding field-cooled data exhibit strong flux expulsion from the sample (Meissner effect) below 28 K, and thus we assign a T_c of 28 K. We have also obtained a 28 K superconductor from the reaction of RbTl with C_{60}, and have detected pure Tl metal after formation of the superconducting phase. Because the same T_c is observed from reaction of C_{60} with Rb, RbHg, and RbTl we believe the only reasonable conclusion is that the identical Rb_yC_{60} superconducting phase is formed in all three reactions. This conclusion is further supported by reactions of KM and CsM (M = Hg, Tl, Bi) with C_{60} that lead to the formation of K_3C_{60} and Cs_xC_{60}, respectively (*12, 16*). Importantly, the superconducting fractions of our powder samples obtained from reaction of 3:1 RbHg (or RbTl):C_{60} are routinely in excess of 35%, and thus suggest that Hg (and Tl) facilitate the incorporation of Rb into the C_{60} lattice to form a homogeneous, bulk superconducting phase.

To assess the global stoichiometry of the superconducting phase we have characterized the fraction of superconductor as a function of the RbHg:C_{60} ratio (Fig. 2). Our data, which were determined from the low-temperature shielding values, show that the maximum superconducting fraction is obtained at a stoichiometry close to 3:1. These results strongly suggest that the stoichiometry of the superconducting phase is Rb_3C_{60}, and thus the Rb- and K-doped superconducting phases have the same stoichiometry. We have also been able to increase the superconducting fraction in sintered pellets. Specifically, pressed and sintered pellets, which were prepared using procedures similar to those reported by Holczer *et al.* (*4*), exhibit low-temperature diamagnetic shielding signals that approach 100% of the theoretical value. Such samples will enable unambiguous magnetic and structural measurements to be made on the Rb-doped superconducting phase.

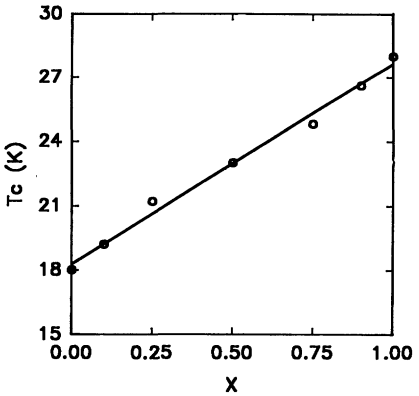

Fig. 4. Plot of T_c versus the Rb:K ratio x in $(Rb_xK_{1-x})_3C_{60}$ materials; the uncertainty in the values of T_c are ±0.2 K.

Because our data now prove that the stoichiometry of the Rb- and K-doped superconducting phases are the same it is important to consider the relationship between these two phases. A classical method to assess experimentally the connectivity between two phases is to study solid solutions, which in the present case correspond to materials with the general formula $(Rb_xK_{1-x})_3C_{60}$. We have prepared these materials using a procedure similar to that employed for the Rb_3C_{60} synthesis. Reaction of $Rb_xK_{1-x}Hg$ alloys with C_{60} in a 3:1 ratio at 200°C produces single-phase superconducting materials in high yields as determined by magnetic susceptibility measurements (Fig. 3). Several important points are evident from these magnetic data. First, analysis of the low temperature shielding values show that the superconducting fractions (x = 0 to 1) are at least 35% for powders; the superconducting fractions of sintered pellets approach 100% (*16*). These data also show no evidence for phase separation (that is, distinct K_3C_{60} and Rb_3C_{60} domains are not formed) within the limits of our sensitivity (0.1 volume percent). Measurements recorded as a function of reaction time further show that rates of Rb and K intercalation must be similar because single-phase materials are obtained for times between 1 and 60 hours. Finally, and perhaps of greatest importance, these data demonstrate that T_c increases systematically with x. As discussed in detail elsewhere (*16*), only Rb and K are incorporated into the C_{60} lattice (for instance, $Rb_xK_{1-x}Tl + C_{60}$ yields similar results), and hence we assign the observed transitions to homogeneous, bulk $(Rb_xK_{1-x})_3C_{60}$ superconducting materials.

We believe that one of the most significant features of our studies is the demonstration of a near linear dependence of T_c with x in these single phase $(Rb_xK_{1-x})_3C_{60}$ materials. These data, which are summarized in Fig. 4, is by no means expected because there has been no clear evidence for mixed alkali-metal intercalation prior to this work. There are several important implications of these new results. First, the continuous evolution of T_c with x in single-phase materials results in the inescapable conclusion that the Rb- and K-doped C_{60} superconducting phases are completely isostructural. Furthermore, these results suggest that there is little preference for Rb versus K occupying the distinct tetrahedral and octahedral sites in the C_{60} lattice (*2, 8*). By way of comparison, it is interesting that the majority of the doping studies of high T_c copper oxide materials have characterized systematic variations in T_c as a function of the hole concentration (*17, 18*). In contrast, our data exhibit a systematic variation in T_c at a constant carrier concentration (assuming that both Rb and K undergo complete charge transfer to C_{60}). We suggest, therefore, that a chemical pressure effect (*19*) provides a viable explanation for these interesting data. Specifically, as x is increased by substituting the larger rubidium ion for K into the solid the lattice expands and the coupling between adjacent C_{60} molecules is reduced; that is, Rb creates a "negative" pressure. This interpretation is supported by recent high-pressure studies of K_3C_{60} which have shown that T_c decreases significantly as the lattice is compressed (*9, 10*). The extreme sensitivity of T_c to pressure, either chemical (this study) or applied externally (*9, 10*), is consistent with a sharply peaked band of electronic states at the Fermi level whose width depends sensitively on the coupling between C_{60} molecules in the lattice.

REFERENCES AND NOTES

1. A. F. Hebard *et al.*, *Nature* **350**, 600 (1991).
2. R. C. Haddon *et al.*, *ibid.*, p. 320.
3. M. J. Rosseinsky *et al.*, *Phys. Rev. Lett.* **66**, 2830 (1991).
4. K. Holczer *et al.*, *Science* **252**, 1154 (1991).
5. P. J. Benning *et al.*, *ibid.*, p. 1417.
6. S. P. Kelty *et al.*, *J. Phys. Chem.*, in press.
7. O. Zhou *et al.*, *Nature* **351**, 462 (1991).
8. P. W. Stephens *et al.*, *ibid.*, p. 632.
9. J. E. Schirber *et al.*, *Physica C*, in press.
10. G. Sparn *et al.*, *Science* **252**, 1829 (1991).
11. K. Holczer *et al.*, *Phys. Rev. Lett.* **67**, 271 (1991).
12. S. P. Kelty, C. C. Chen, C. M. Lieber, *Nature* **352**, 223 (1991).
13. W. Krätschmer *et al.*, *ibid.* **347**, 254 (1990).
14. R. E. Haufler *et al.*, *J. Phys. Chem.* **94**, 8634 (1990).
15. F. Diederich *et al.*, *Science* **252**, 548 (1991).
16. S. P. Kelty, C. C. Chen, C. M. Lieber, in preparation. Tl metal has been detected by x-ray diffraction following reaction of MTl with C_{60}, and thus shows that it is not substituted into the C_{60} lattice under these conditions. Additionally, diffraction studies show that K_3C_{60} and Rb_3C_{60} have similar fcc (face-centered-cubic) lattices.
17. R. J. Cava, *Science* **247**, 656 (1990).
18. M.-H. Whangbo and C. C. Torardi, *Acc. Chem. Res.* **24**, 127 (1991).
19. J. M. Williams *et al.*, *Prog. Inorg. Chem.* **35**, 51 (1987).

18 July 1991; accepted 31 July 1991

Interpretation of Snow-Climate Feedback as Produced by 17 General Circulation Models

R. D. Cess, G. L. Potter, M.-H. Zhang, J.-P. Blanchet, S. Chalita, R. Colman, D. A. Dazlich, A. D. Del Genio, V. Dymnikov, V. Galin, D. Jerrett, E. Keup, A. A. Lacis, H. Le Treut, X.-Z. Liang, J.-F. Mahfouf, B. J. McAvaney, V. P. Meleshko, J. F. B. Mitchell, J.-J. Morcrette, P. M. Norris, D. A. Randall, L. Rikus, E. Roeckner, J.-F. Royer, U. Schlese, D. A. Sheinin, J. M. Slingo, A. P. Sokolov, K. E. Taylor, W. M. Washington, R. T. Wetherald, I. Yagai

Snow feedback is expected to amplify global warming caused by increasing concentrations of atmospheric greenhouse gases. The conventional explanation is that a warmer Earth will have less snow cover, resulting in a darker planet that absorbs more solar radiation. An intercomparison of 17 general circulation models, for which perturbations of sea surface temperature were used as a surrogate climate change, suggests that this explanation is overly simplistic. The results instead indicate that additional amplification or moderation may be caused both by cloud interactions and longwave radiation. One measure of this net effect of snow feedback was found to differ markedly among the 17 climate models, ranging from weak negative feedback in some models to strong positive feedback in others.

The most comprehensive way to infer future climate change, caused by increasing greenhouse gases, is by means of three-dimensional general circulation models (GCMs). The climate responses of existing GCMs, however, to increasing atmospheric CO_2 differ considerably (*1*), as is consistent with a GCM intercomparison study that addressed two interactive climate feedback mechanisms: water vapor feedback and cloud feedback (*2, 3*). The former is a positive feedback because climate warming produces an increase in atmospheric water vapor, itself a greenhouse gas, that amplifies